

# On Radial and Angular Correlations in a Confined System of Two Atoms in a Two-Dimensional Geometry

Przemysław Kościk<sup>1, \*</sup>

<sup>1</sup>Department of Computer Sciences, University of Applied Sciences, Mickiewicza 8, PL-33100 Tarnów, Poland

We study the ground-state correlations between two atoms in an isotropic two-dimensional harmonic trap with finite-range soft-core interactions. Our study shows that in the case of repulsive forces, the wave function can be approximated as the product of the radial and angular components, regardless of the range of the interaction. This allows the separation of particle correlations into radial and angular correlations, which can be analyzed independently. However, there are still correlations in each subsystem that are strongly dependent on the system parameters. The results show that radial correlations are generally weaker than angular correlations. We have also made some observations about particle correlations in the case of attraction.

**INTRODUCTION.**— In recent years, there has been a growing interest in studying the properties of systems consisting of particles confined in external potentials [1–15]. This interest has been fuelled by significant experimental advances that make it possible to create such systems in the laboratory. Entanglement in these systems has received considerable attention because of its relevance to quantum information technology and the challenge of quantifying the degree of correlation. In particular, considerable scientific effort has been devoted to understanding the correlation properties of harmonically trapped systems, including those with harmonic [16], delta-contact [17, 18], finite-range soft-core [19], inverse power-law [20–24], and  $\wp$ -wave interactions [15, 17]. Several studies have also explored entanglement in natural systems such as helium and helium-like atoms [25–28]. A review of entanglement in composite systems, including atoms and molecules, can be found in [29]. In addition, recent advances in machine learning and deep learning are opening up new opportunities to study entanglement properties in various quantum systems [30, 31], including few-body systems [32–34]

The goal of our research is to better understand the correlation properties of a two-dimensional system consisting of two bosonic atoms in a harmonic trapping potential and interacting through a finite-range soft-core potential. The Hamiltonian that describes this system is given by

$$\mathcal{H} = \sum_{i=1}^2 \left[ -\frac{\hbar^2 \nabla_{\mathbf{r}_i}^2}{2m} + V(\mathbf{r}_i) \right] + U(|\mathbf{r}_1 - \mathbf{r}_2|), \quad (1)$$

with  $V(\mathbf{r}) = m\omega^2 \mathbf{r}^2/2$  and

$$U(\mathbf{r}) = \begin{cases} \kappa, & 0 \leq r \leq \sigma \\ 0, & r > \sigma, \end{cases} \quad (2)$$

where  $\kappa$  and  $\sigma$  are the strength and range of the interaction, respectively. The potential (2) has been used

to simulate various atomic systems [35–39], including those with Rydberg-dressed atoms [40–43]. The advantage of this system is that it can be solved exactly [44, 45] with solutions expressed by special functions. Closed-form analytical solutions are available for certain values of the control parameters [45].

We will present our results in the following order. First, we analyze the correlations between the atoms. Then, we will examine the correlations between subsystems associated with radial and angular variables. Finally, we will examine the radial and angular correlations, emphasizing the hardcore limit  $\kappa \rightarrow \infty$  to keep the discussion concise. The conclusions highlight the main findings of the study.

**PARTICLE CORRELATIONS.**— The ground state is the  $S$  symmetry state, which depends on the radial coordinates  $r_1$  and  $r_2$  and the interparticle angular coordinate  $\theta_{12} = \varphi_1 - \varphi_2$ . A tool for analyzing the correlations between two bosonic atoms is the Schmidt decomposition [46]. To derive the Schmidt formula for the  $S$  state wave function, we first decompose the function  $\Psi$  into a Fourier-Lagrange series

$$\sqrt{r_1 r_2} \Psi(\mathbf{r}_1, \mathbf{r}_2) = \frac{g_0(r_1, r_2)}{2\pi} + \sum_{l=1}^{\infty} \frac{g_l(r_1, r_2) \cos[l(\varphi_1 - \varphi_2)]}{\pi}, \quad (3)$$

where the term  $\sqrt{r_1 r_2}$  provides the correct normalization in the radial directions, and the component  $g_l(r_1, r_2)$  is calculated using the integral

$$g_l(r_1, r_2) = \sqrt{r_1 r_2} \int_0^{2\pi} d\theta_{12} \Psi(\mathbf{r}_1, \mathbf{r}_2) \cos(l\theta_{12}). \quad (4)$$

After obtaining the Schmidt form:

$$g_l(r_1, r_2) = \sum_{n=0}^{\infty} k_{nl} \chi_{nl}(r_1) \chi_{nl}(r_2), \quad (5)$$

we use the identity  $\cos(l\theta_{12}) = (e^{il\theta_{12}} + e^{-il\theta_{12}})/2$  to represent the total wave function  $\Psi$  as:

$$\Psi(\mathbf{r}_1, \mathbf{r}_2) = \sum_{\substack{n=0 \\ l=-\infty \dots \infty}} k_{nl} u_{nl}^*(\mathbf{r}_1) u_{nl}(\mathbf{r}_2). \quad (6)$$

\* p.koscik@pwsztar.edu.pl

Single particle orbitals

$$u_{nl}(\mathbf{r}) = \frac{\chi_{nl}(r)}{\sqrt{r}} \frac{e^{il\varphi}}{\sqrt{2\pi}}, \quad (7)$$

form an orthonormal basis set, i.e.,  $\int_0^{2\pi} \int_0^\infty d\varphi dr [r u_{nl}^*(\mathbf{r}) u_{n'l'}(\mathbf{r})] = \delta_{nn'} \delta_{ll'}$  ( $k_{nl} = k_{n|l|}$ ,  $\chi_{nl}(r) = \chi_{n|l|}(r)$ ). As a result, we can recognize the expansion in Eq. (6) as the Schmidt decomposition of the  $S$ -state wave function. Note that both the orbital  $u_{nl}(\mathbf{r})$  and its complex conjugate are eigenfunctions of the angular momentum operator ( $-i\hbar\partial_\varphi$ ), and the spatial reduced density matrix (RDM),

$$\rho(\mathbf{r}, \mathbf{r}') = \int \Psi^*(\mathbf{r}, \mathbf{r}_2) \Psi(\mathbf{r}', \mathbf{r}_2) d\mathbf{r}_2, \quad (8)$$

that is,

$$\rho(\mathbf{r}, \mathbf{r}') = \sum_{n=-\infty \dots \infty} \lambda_{nl} u_{nl}(\mathbf{r}) u_{nl}^*(\mathbf{r}'), \quad (9)$$

with the eigenvalues  $\lambda_{nl}$  (occupancies) related to the Schmidt coefficients  $k_{nl}$  by  $\lambda_{nl} = k_{nl}^2$ . All occupancies except those with  $l = 0$  are doubly degenerate. The state of two bosonic atoms is nonentangled if and only if it can be represented by a single permanent (the counterpart of the Slater determinant in the case of fermions) [46].

To quantify the degree of correlation, which indicates the deviation from an unentangled state, we use a participation ratio  $K = \mathcal{P}^{-1}$  [47], where  $\mathcal{P}$  is the purity of the RDM  $\mathcal{P} = \text{Tr} \rho^2$ . The participation measures the average number of one-particle orbitals actively involved in the Schmidt decomposition of the RDM. The purity  $\mathcal{P}$  can be expressed as

$$\mathcal{P} = \sum_l \int [\rho_l(r, r')]^2 dr dr' = \sum_{nl} \lambda_{nl}^2, \quad (10)$$

where  $\rho_l(r, r') = \int g_l(r, r_2) g_l(r', r_2) dr_2$ . The quantity that provides additional insight into the correlations is the so-called collective occupancy, which is defined as follows:

$$f_l = \tilde{\delta}_l \int \rho_l(r, r) dr = \tilde{\delta}_l \sum_n \lambda_{nl}, l \geq 0, \quad (11)$$

where  $\tilde{\delta}_0 = 1$  and  $\tilde{\delta}_l = 2$  in opposite cases,  $\sum_l f_l = 1$ . We can interpret the value of  $f_l$  as the probability of finding pairs of particles with zero ( $l = 0$ ) and opposite angular momenta  $-\hbar l$  and  $\hbar l$  ( $l > 0$ ).

Fig. 1 summarizes our results for particle correlations in the ground state. In the left panel, we can see the results obtained in the hardcore limit  $\kappa \rightarrow \infty$  as a function of  $\sigma$ . The plots labeled (a) and (b) represent the results for the participation ratio and the corresponding

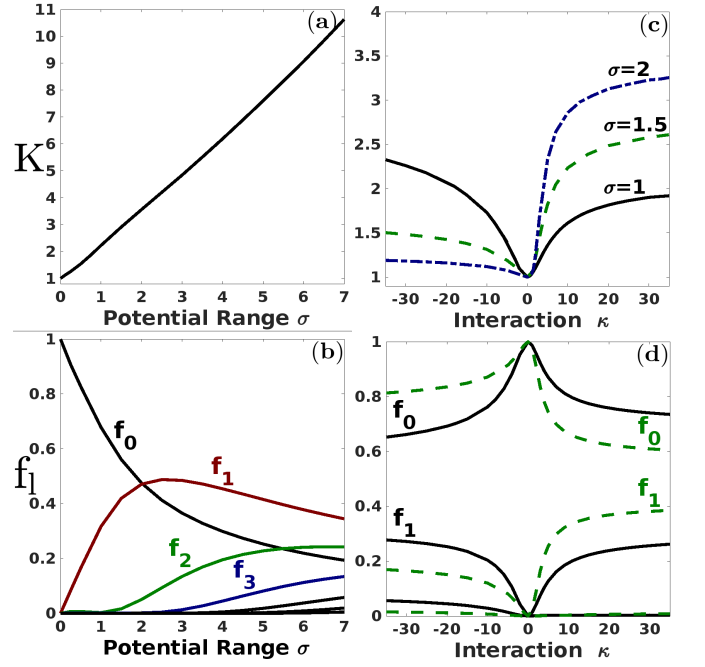


FIG. 1. The graphs labeled (a) and (b) depict the participation ratio  $K$  and the collective occupancies  $f_l$  as functions of  $\sigma$  in the hardcore limit ( $\kappa \rightarrow \infty$ ), respectively. Graph (c) illustrates the participation ratio  $K$  for three different values of  $\sigma$  as functions of  $\kappa$ . Plot (d) shows the collective occupancies  $f_l$  for  $\sigma$  equal to 1 and  $3/2$  as functions of  $\kappa$ . The range and strength of the interactions are measured in  $\sqrt{\hbar/m\omega}$  and  $\hbar\omega$ , respectively.

collective occupancies, respectively. The participation ratio grows almost linearly with increasing  $\sigma$ , indicating that the number of significant Schmidt orbitals in Eq. (6) also increases similarly. The fraction of particle pairs with only radial correlations ( $f_0$ ) decreases steadily with  $\sigma$ . In contrast, the collective occupancies with higher values of  $l$  show a more complicated behavior. Initially, the value of the collective occupancy  $f_1$  increases with increasing  $\sigma$ , reaching parity with  $f_0$  around  $\sigma = 2$ . Beyond this point, the contribution of  $f_1$  decreases, and the components with higher  $l$  become more prominent, indicating more complex correlation effects.

We have found that if  $f_l$  is significant, then  $g_l(r_1, r_2)$  can be approximated as  $g_l(r_1, r_2) \approx k_{0l} \chi_{0l}(r_1) \chi_{0l}(r_2)$ . This result suggests that the number of important Schmidt orbitals in the expansion in Eq. (6) (represented by  $K$ ) is approximately related to the number of essential collective occupancies (denoted by  $\eta$ ) via  $K \approx 2\eta - 1$ . Fig. 1 (a) and (b) provide evidence for this relationship. The right panel of Fig. 1 shows the results obtained for finite interaction strengths  $\kappa$ . We observe that the effect of varying  $\sigma$  on the correlations in the attraction regime is opposite to that in the repulsion regime. It is worth noting that increasing  $\sigma$  for attractive forces leads to a significant expansion of the range of  $\kappa$  where entanglement is weak. The considered state becomes nearly unentangled ( $K \approx 1$ ) over a wide range

of negative  $\kappa$  starting from  $\sigma = 2$ .

**RADIAL AND ANGULAR CORRELATIONS.**— To analyze the correlations between the subsystems associated with the radial  $\vec{r} = (r_1, r_2)$  and angular  $\vec{\varphi} = (\varphi_1, \varphi_2)$  variables, we use the Schmidt formula in the following form:

$$\sqrt{r_1 r_2} \Psi(\mathbf{r}_1, \mathbf{r}_2) = \sum_n \tilde{k}_n \mathcal{V}_n(\vec{r}) \Phi_n(\vec{\varphi}). \quad (12)$$

Using the singular value decomposition theorem, we obtain

$$\mathcal{V}_n(\vec{r}) = \sum_j (\mathbf{V})_{jn} v_j(\vec{r}), \quad (13)$$

and

$$\Phi_n(\vec{\varphi}) = \sum_j (\mathbf{U})_{jn} \Theta_j(\vec{\varphi}), \quad (14)$$

with

$$\Theta_0(\vec{\varphi}) = \frac{1}{2\pi}, \Theta_j(\vec{\varphi}) = \frac{\cos[j(\varphi_1 - \varphi_2)]}{\sqrt{2\pi}}, \quad (15)$$

where  $\mathbf{M} = \mathbf{U}\mathbf{Q}\mathbf{V}^T$ , and  $\mathbf{M} = [M_{lm}]$  is a matrix with entries  $M_{lm} = \sqrt{\tilde{\delta}_l} \int g_l(r_1, r_2) v_m(\vec{r}) dr_1 dr_2$ . Here,  $\{v_m(\vec{r})\}$  denotes a set of orthonormal basis functions, and  $\tilde{k}_n = \mathbf{Q}_{nn}$  and  $\tilde{\delta}_l$  are defined below Eq. (11). The conservation of probability gives  $\sum_n \tilde{k}_n^2 = 1$ . In our calculations, we use a basis set consisting of the permanents  $v_m(\vec{r}) = \text{per}[\tilde{v}_{m_1}(r_1), \tilde{v}_{m_2}(r_2)]$  formed by single particle orbitals  $\tilde{v}_s(r) = \sqrt{2/L} \sin(s\pi r/L)$ . We choose the size of the radial box  $L$  to ensure that the region containing the functions  $g_l(r_1, r_2)$  is covered by the permanents  $v_m(\vec{r})$ .

To keep it short, we focus primarily on the  $\kappa \rightarrow \infty$  limit. Our results indicate that the value of  $\tilde{\lambda}_0 = \tilde{k}_0^2$  is very close to 1, regardless of the value of the interaction range  $\sigma$ . This phenomenon is illustrated in Fig. 2 (a), which shows the behavior of  $\tilde{\lambda}_0$  as a function of  $\sigma$ . We observe an intriguing feature: a minimum around  $\sigma = 0.9$ . As a result, we can conclude that the wave function  $\Psi$  can be approximated as

$$\sqrt{r_1 r_2} \Psi(\mathbf{r}_1, \mathbf{r}_2) \approx \mathcal{V}_0(r_1, r_2) \Phi_0(\varphi_1, \varphi_2), \quad (16)$$

which indicates almost no correlations between the radial and angular subsystems. However, there are still correlations present within each subsystem, as shown in Fig. 2 (b) and Fig. 2 (c), which depict the participation ratios calculated for the radial and angular orbitals  $\mathcal{V}_0(r_1, r_2)$  and  $\Phi_0(\varphi_1, \varphi_2)$ , denoted by  $K_{\vec{r}}$  and  $K_{\vec{\varphi}}$ , respectively. Note that diagonalization is necessary to obtain the Schmidt form of  $\mathcal{V}_0(r_1, r_2)$ . In contrast, the function  $\Phi_0(\varphi_1, \varphi_2)$  can be automatically written in Schmidt form as follows

$$\Phi_0(\varphi_1, \varphi_2) = \sum_{l=\dots, -2, -1, 0, 1, 2, \dots} w_l \phi_l^*(\varphi_1) \phi_l(\varphi_2), \quad (17)$$

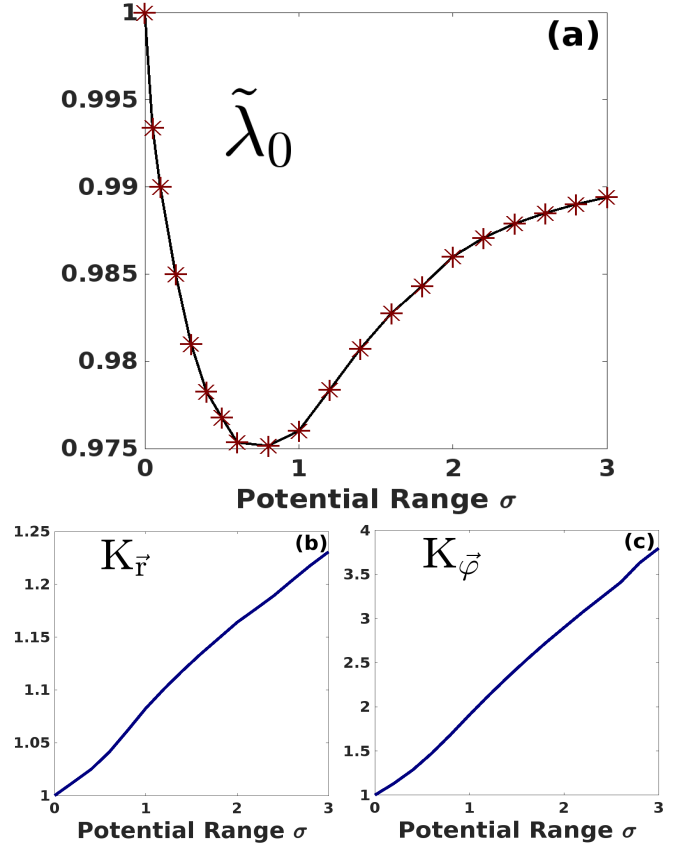


FIG. 2. Results obtained in the hardcore interaction limit ( $\kappa \rightarrow \infty$ ) as a function of  $\sigma$ . Graph (a) shows the behavior of  $\tilde{\lambda}_0 = \tilde{k}_0^2$ . Plots (b) and (c) show the behavior of the participation ratios of both  $K_{\vec{r}}$  and  $K_{\vec{\varphi}}$ , respectively.

where  $\phi_l(\varphi) = e^{il\varphi}/\sqrt{2\pi}$  and  $w_l = \tilde{\delta}_l^{-1/2} (\mathbf{U})_{|l|0}$  ( $\tilde{\delta}_0 = 1$ ,  $\tilde{\delta}_l = 2$ ), and the participation ratio  $K_{\vec{\varphi}}$  can be calculated as  $K_{\vec{\varphi}} = \sum_l w_l^4$ . As shown in Fig. 2, the radial correlations are generally weaker than the angular correlations. The difference in their magnitudes is obvious and becomes more pronounced as the value of  $\sigma$  increases. Through thorough testing, we have verified that Eq. (16) remains valid even when there are finite repulsive forces  $\kappa$ . Deviations were observed only in the presence of attraction, but we will not go into detail here.

Sample results for radial and angular distributions:  $n(r_1, r_2) = \int r_1 r_2 |\Psi|^2 d\vec{\varphi}$  and  $\Gamma(\varphi_1, \varphi_2) = \int r_1 r_2 |\Psi|^2 d\vec{r}$  can be found in [45]. Based on our current results, we can conclude that in the case of repulsion:  $n(r_1, r_2) \approx |\mathcal{V}_0(r_1, r_2)|^2$  and  $\Gamma(\varphi_1, \varphi_2) \approx |\Phi_0(\varphi_1, \varphi_2)|^2$ . It is worth mentioning that the system undergoes crystallization, which is evident from the appearance of a distinct peak in the orbital  $\Phi_0(\varphi_1, \varphi_2)$  at  $\theta_{12} \approx \pi$ . As we have checked, the width of the peak decreases with increasing  $\sigma$ , indicating the improved localization of atoms on opposite sides of the trap.

**CONCLUSIONS.**— We comprehensively analyzed the correlations between two bosonic atoms confined in a harmonic trap and interacting through a finite-range soft-core potential. To this end, we derived Schmidt formulas that allowed us to quantify the correlations between the particles and the subsystems associated with their radial and angular variables. The main discovery of our study is that when there is repulsion between the particles, the correlations between them are split into ra-

dial and angular correlations. This study contributes to our overall understanding of quantum correlations between confined particles. The results suggest that studying the effects of factors such as the confinement potential, the type of interaction, and the number of particles on the correlations between the radial and angular subsystems could improve our understanding of these correlations in the generation of different quantum states.

- 
- [1] M. A. Załuska-Kotur, M. Gajda, A. Orłowski, and J. Mostowski, *Phys. Rev. A* 61, 033613 (2000)
- [2] A. Minguzzi, M. D. Girardeau, *Phys. Rev. A* 73, 063614 (2006)
- [3] K. Sakmann, A. I. Streltsov, O. E. Alon, and L. S. Cederbaum, *Phys. Rev. A* 78, 023615 (2008)
- [4] D. Delande, K. Sacha, M. Płodzień, S. K. Avazbaev, J. Zakrzewski, *New J. Phys.* 15, 045021 (2013)
- [5] A. Dawid, M. Lewenstein, and M. Tomza, *Phys. Rev. A* 97, 063618 (2018)
- [6] P. Kościk, M. Płodzień, and T. Sowiński, *Europhysics Letters*, 123, 36001 (2018)
- [7] T. Sowiński, M. Á. García-March, *Rep. Prog. Phys.* 82, 104401 (2019)
- [8] S. Bera, B. Chakrabarti, A. Gammal, M. C. Tsatsos, M. L. Lekala, B. Chatterjee, C. Lévêque, and A. U. J. Lode, *Sci Rep* 9, 17873 (2019)
- [9] G. Bougas, S. I. Mistakidis, G. M. Alshalan, and P. Schmelcher, *Phys. Rev. A* 102, 013314 (2020)
- [10] S. I. Mistakidis, A. G. Volosniev, and P. Schmelcher, *Phys. Rev. Research* 2, 023154 (2020)
- [11] F. Brauneis, T. G. Backert, S. I. Mistakidis, M. Lemesko, H-W Hammer, and A. G. Volosniev, *New J. Phys.* 24, 063036 (2022)
- [12] M. Suchorowski, A. Dawid, and M. Tomza, *Phys. Rev. A* 106, 043324 (2022)
- [13] A. Syrwid, M. Łebek, P. T. Grochowski, and K. Rzążewski, *Phys. Rev. A* 105, 013314 (2022)
- [14] B. Parajuli, D. Pećak, and C-C Chien, *Phys. Rev. A* 107, 023308 (2023)
- [15] P. Kościk, T. Sowiński, *Phys. Rev. Lett.* 130, 253401 (2023)
- [16] P. A. Bouvrie, A. P. Majtey, A. R. Plastino, P. Sánchez-Moreno, and J. S. Dehesa, *Eur. Phys. J. D* 66, 15 (2012)
- [17] B. Sun, D. L. Zhou, and L. You, *Phys. Rev. A* 73, 012336 (2006)
- [18] M. Płodzień, D. Wiater, A. Chrostowski, T. Sowiński, *arXiv:1803.08387 [cond-mat]* (2018)
- [19] P. Kościk, T. Sowiński, *Sci Rep* 8, 48 (2018)
- [20] P. Kościk, *Phys. Lett. A* 379 (4), 293-298 (2015)
- [21] M. Garagiola, E. Cuestas, F. M. Pont, P. Serra, and O. Osenda, *Phys. Rev. A* 94, 042115 (2016)
- [22] O. Osenda, F. M. Pont, A. Okopińska, and P. Serra, *J. Phys. A: Math. Theor.* 48 485301 (2015)
- [23] P. Kościk, *Eur. Phys. J. D* 71, 286 (2017)
- [24] E. Cuestas, P. A. Bouvrie, and A. P. Majtey, *Phys. Rev. A* 101, 033620 (2020)
- [25] J. S. Dehesa, T. Koga, R. J. Yáñez, A. R. Plastino, and R. O. Esquivel, *J. Phys. B At. Mol. Opt. Phys.* 45, 015504 (2012)
- [26] G. Benenti, A. Siccardi, G. Strini, *Eur. Phys. J. D.* 67, 83 (2013)
- [27] Y. C. Lin, C. Y. Lin, Y. K. Ho, *Phys. Rev. A* 87, 022316 (2013)
- [28] Z. Huang, H. Wang, S. Kais, *J. Mod. Opt.* 53, 2543 (2006)
- [29] M. C. Tichy, F. Mintert, and A. Buchleitner, *J. Phys. B: At. Mol. Opt. Phys.* 44, 192001 (2011)
- [30] A. Dawid, J. Arnold, B. Requena, A. Gresch, M. Płodzień, K. Donatella, K. A. Nicoli, P. Stornati, R. Koch, M. Büttner, R. Okuła, G. Muñoz-Gil, R. A. Vargas-Hernández, A. Cervera-Lierta, J. Carrasquilla, V. Dunjko, M. Gabrié, P. Huembeli, E. van Nieuwenburg, F. Vicentini, L. Wang, S. J. Wetzel, G. Carleo, E. Greplová, R. Krems, F. Marquardt, M. Tomza, M. Lewenstein, A. Dauphin, *arXiv:2204.04198 [quant-ph]* (2022)
- [31] A. M. Palmieri, G. Müller-Rigat, A. K. Srivastava, M. Lewenstein, G. Rajchel-Mieldzioć, and M. Płodzień, *arXiv:2309.10616 [quant-ph]* (2023)
- [32] JWT. Keeble, M. Drissi, A. Rojo-Francàs, B. Juliá-Díaz, A. Rios, *arXiv:2304.04725 [nucl-th]*(2023)
- [33] J. Kessler, F. Calcavecchia, and T. D. Kühne, *Adv. Theory Simul.* 4, 2000269 (2021)
- [34] P. F. Bedaque, H. Kumar, A. Sheng, *arXiv:2309.02352 [nucl-th]* (2023)
- [35] K. Barkan, M. Engel, and R. Lifshitz, *Phys. Rev. Lett.* 113, 098304 (2014)
- [36] P. Kroiss, M. Boninsegni, and L. Pollet, *Phys. Rev. B* 93, 174520 (2016)
- [37] P. Mujal, E. Sarlé, A. Polls, and B. Juliá-Díaz, *Phys. Rev. A* 96, 043614 (2017)
- [38] P. Mujal, A. Polls, and B. Juliá-Díaz, *Phys. Rev. A* 101, 043619 (2020)
- [39] M. Imran and M. A. H. Ahsan, *J. Phys. B: At. Mol. Opt. Phys.* 53, 125303 (2020)
- [40] J. Honer, H. Weimer, T. Pfau, and H. P. Büchler, *Phys. Rev. Lett.* 105, 160404 (2010)
- [41] N. Henkel, R. Nath, and T. Pohl, *Phys. Rev. Lett.* 104, 195302 (2010)
- [42] M. Płodzień, G. Lochead, J. de Hond, N. J. van Druten, and S. Kokkelmans, *Phys. Rev. A* 95, 043606 (2017)
- [43] M. Płodzień, T. Sowiński, and S. Kokkelmans, *Sci Rep* 8, 9247 (2018)
- [44] D. Saraidaris, I. Mitrakos, I. Brouzos, and F. Diakonou, *arXiv:1903.08499 [quant-ph]* (2019).
- [45] P. Kościk, T. Sowiński, *Sci Rep* 9, 12018 (2019)
- [46] G. Ghirardi and L. Marinatto, *Phys. Rev. A* 70, 012109 (2004)
- [47] R. Grobe, K Rzążewski, and J. H. Eberly, *J. Phys. B: At. Mol. Opt. Phys.*, 27, 16, pp. L503-L508 (1994)